

Carbonation and corrosion of steel in fly ash concrete, concluding investigation of five-year-old laboratory specimens and preliminary field data

Andres Belda Revert^{a,b,*}, Tobias Danner^c, Mette Rica Geiker^a

^a Norwegian University of Science and Technology, Department of Structural Engineering, Trondheim, Norway

^b OPAK AS, Department of Construction Specialist Advise, Oslo, Norway

^c Sintef, Department of architecture, materials and structures, Trondheim, Norway

ARTICLE INFO

Keywords:

Concrete
Fly ash
Carbonation
Reinforcement corrosion

ABSTRACT

Carbonation development and reinforcement corrosion were investigated on concretes exposed for a five-year period at 90% RH, 20 °C, and 5% CO₂, and for a six-year period at natural carbonation. Portland cement-based binders with 0%, 18%, and 30% fly ash were investigated. The fly ash blends showed lower carbonation resistance compared to PC both at laboratory and field exposure, a large difference in carbonation performance was observed between the laboratory exposed specimens. The carbonation rate was fastest on the laboratory specimens and showed square-root time dependency the first 2.5 years, but reduced rate at later age. Deeper carbonation depths were in general observed in the vicinity of the reinforcement compared to the unreinforced laboratory exposed specimens. Not all specimens were fully carbonated at the steel-concrete interface. The correlation between degree of carbonation of the steel-mortar interface, the open circuit potential, and the observed corrosion of the steel bars varied between binders and bar position (top or bottom). The measured corrosion rate in the laboratory exposed (90% RH, 20 °C, and 5% CO₂) carbonated concrete was on average 0.2 μA/cm², with an upper value of 0.6 μA/cm². The highest corrosion rate was measured in the fly ash concrete. No corrosion rate data are yet available for the field exposed concretes.

1. Introduction

Global process emissions from the cement industry were in 2018 equivalent to about 4% of emissions from fossil fuels [1]. The CO₂ footprint of the cement industry can be reduced by substituting part of the Portland cement (PC) by supplementary cementitious materials (SCMs), e.g., fly ash from coal fired power plants. Since the 80's such fly ash has been used in Norway as SCM [2], typically in form of CEM II/A-V (M) with ca. 18% fly ash replacement [3]. In general, blended cements present advantages compared to Portland cement. However, a main drawback is the lower carbonation resistance.

The design service life of a reinforced concrete structure is defined by a limit state and the level of reliability (or probability of failure) for not passing it [4]. The service life of reinforced concrete structures is typically divided into two periods, the initiation and propagation periods. The initiation period is the time interval during which detrimental substances penetrate the cover until active corrosion can be sustained. In

the propagation period damage (e.g., corrosion) develops until an unacceptable level of deterioration. For carbonating reinforced concrete structures depassivation of the steel reinforcement is the limit state typically used for service life design [4]. However, carbonation of the steel-concrete interface is not the only prerequisite for active corrosion. Depending on the availability of moisture, the propagation period might indeed consist of periods with active corrosion and periods with passive corrosion [5].

While much literature is addressing the mechanisms and rate of carbonation of blended cements [6], studies on the effect of SCM on reinforcement corrosion are in comparison limited [5].

Corrosion rates in carbonated concrete vary over various orders of magnitude. Recent literature reviews summarize reported corrosion rates in carbonated concrete [7,8]. A large scatter was registered, from values in the range of 0.002 to 20 μA/cm², (0.08 to 2 μA/cm² when considering average values) [7,8]. Data on corrosion rate at 90% humidity is limited, with reported values from 0.2 to 3 μA/cm² for mortar

* Corresponding author.

E-mail address: abr@opak.no (A.B. Revert).

or concrete made from ordinary Portland cement (w/b 0.47-0.9), early strength Portland cement (w/b=0.55), and blast furnace slag (w/b=0.55) [7,8].

A recent study investigated corrosion in blended cements [9]. Binders with 0% (PC) and 30% fly ash (FA) were investigated among other materials. The specimens were prepared with w/c 0.6, cured for 7 days at 95% RH and 20 °C, and carbonated at 100% CO₂. The specimens were subsequently exposed to different moisture and temperature conditions in laboratory environment. At 90% RH and 20 °C, corrosion rate of about 0.04 μA/cm² were measured on PC, and 0.1 μA/cm² on FA specimens. The open circuit potential (OCP) oscillated between -100 to -350 mV for PC, and -200 to -300 mV for FA (vs SCE). Comparable electrical resistivity was measured on carbonated PC and FA specimens.

The aim of this investigation was to quantify the impact of fly ash on carbonation induced reinforcement corrosion in concrete, and gather data for service life modelling, both for the initiation and the propagation period. Reinforced and unreinforced specimens were kept at constant laboratory conditions of 90% RH, 20 °C and 5% CO₂, and wall elements were exposed to natural carbonation in a rural field station in Trondheim, Norway. Within the five years period, corrosion was only observed in the laboratory exposed reinforced specimens, which were opened to allow comparison of measured values and actual carbonation and corrosion state.

2. Experimental

2.1. Specimens

Reinforced and unreinforced concrete specimens were prepared for laboratory exposure, and wall elements were prepared for field exposure. All specimens were cast at the same time using the same concrete mixes. Three different cements with 4% limestone filler and varying amount of fly ash (0, 18%, and 30%), were used, all provided by Heidelberg Materials Sement Norge AS. The fly ash is category A according to NS-EN 450-1 [10], with a CaO content of 5% in mass [11]. This corresponds to ASTM Class F (low CaO fly ash) [12].

The chemical composition of the three different cements is given in Table 1, and the compositions of the concretes are summarized in Table 2. The cements were blended in a cement factory, thus the term “cement” is applicable. The target w/c was 0.55, but some variations were registered.

2.1.1. Laboratory specimens

Unreinforced concrete specimens (120×120×260 mm) were prepared for investigating the carbonation development, while reinforced specimens (320×300×120 mm) were prepared for investigating corrosion initiation and propagation. Each reinforced specimen contained six carbon steel reinforcement bars: three at the bottom (#1- 3) and three at the top (#4-6), see Fig. 1. The reinforced specimens were instrumented and contained two counter electrodes made from stainless steel bars (SS1 and SS2 in Fig. 1), one embedded reference electrode type ERE 20, and one pseudo-reference electrode made from a piece of titanium mesh (Ti in Fig. 1).

All reinforcement bars were made from ribbed carbon steel diameter (B 500 NC), 16 mm in diameter, and had a 20 mm concrete cover. The reinforcement was used in “as received” condition. The reinforcement was cut into ca. 300 mm pieces and the ends were polished. Both ends of

Table 1

Chemical composition of the cements, determined by XRF.

Cement type	SiO ₂	Al ₂ O ₃	Fe ₂ O ₃	CaO	MgO	SO ₃	P ₂ O ₅	K ₂ O	Na ₂ O
CEM I	19.6	4.9	3.1	60.8	2.3	3.7	0.1	0.9	0.5
CEM II/B-M*	25.5	7.6	4.2	50.7	2.1	3.3	0.2	1.1	0.6
CEM II/B-V	28.4	8.8	4.4	46.9	2.2	2.7	0.2	1.2	0.6

* According to the supplier [13]

Table 2

Concrete compositions [kg/m³]. Aggregates in saturated-surface dry condition.

Constituent	PC	18% FA	30% FA
Cement type (see Table 1)	CEM I	CEM II/B-M	CEM II/B-V
Cement	371.4	369.8	369.5
Sand 0/8 mm	1173.2	1166.9	1160.3
Gravel 5/16 mm	624.2	628.5	629.6
Free water	206.9	202.9	200.9
Superplasticiser	3.78	3.69	3.68
w/c	0.56	0.55	0.54

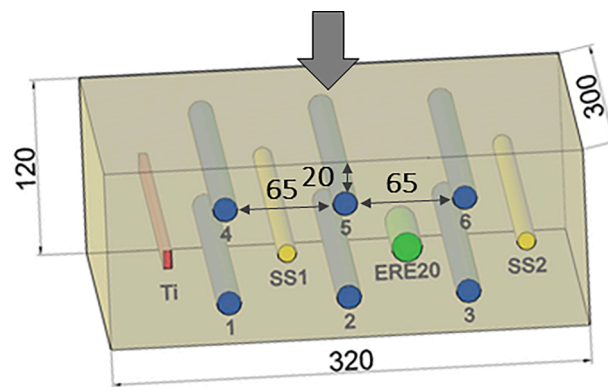


Fig. 1. Sketch of reinforced concrete specimen for laboratory exposure containing six Ø16 mm reinforcement (three at the bottom (#1- 3) and three at the top (#4-6)), two counter electrodes (stainless steel bars, SS1 and SS2), one reference electrode (ERE20), and one pseudo-reference electrode (Ti). The arrow from the top shows the casting direction. All measures are in mm.

the bars were coated with beeswax to a length of 50 mm in order to prevent corrosion at the ends of the bars. The reinforcement was cleaned with acetone to remove possible grease and kept in a desiccator including a drying agent (silica gel) until they were embedded in concrete.

The concretes were prepared at a pre-cast concrete plant in batches of ca. 1 m³. The concrete was poured into the moulds and gently compacted by tapping on the sides of the mould until no air bubbles appeared on the surface for the laboratory specimens. The moulds were covered with plastic and kept at 20 °C. The specimens were demoulded after 3 days and subsequently cured for 11 days at 20 °C wrapped in plastic. After curing, the specimens were exposed to 90 ± 2% RH, 20 °C, and 5 ± 0.1% CO₂ for five years. Climate cabinets with forced ventilation were used to ensure homogeneous exposure conditions. The aim of this exposure condition was to use an environment with a well-defined (constant) humidity, which promotes both carbonation and corrosion development.

2.1.2. Field specimens

Non-reinforced and instrumented reinforced wall elements (1500×1300×250 mm) were prepared from each type of concrete.

Ribbed carbon steel diameter 16 mm (B 500 NC) was used as reinforcement. Two meshes of reinforcement with horizontal and vertical bars were embedded with a 20-mm cover in each element. Cables that allow to electrically connect or disconnect each horizontal bar from the

rest of the reinforcement depending on the necessities were installed. Each wall element contained six electrically isolated horizontal reinforcement bars on each side (#1-6 from bottom to top). The vertical bars of each layer were electrically connected.

Three sets of three reference electrodes type ERE 20 were embedded in the middle of each wall element. The reference electrodes are marked in green colour in Fig. 2 (left and middle).

Resistivity probes were prepared by sandblasting smooth steel reinforcement, 10 mm in diameter, and placing them with a given distance. Six sets of three probes were embedded in each wall element between the two meshes of reinforcement. The resistivity probes have a concrete cover of 5 cm on each side. The resistivity probes are marked in blue colour in Fig. 2, left and middle.

The concretes were prepared at a pre-cast concrete plant in batches of ca. 1 m³. The concrete was poured into the moulds and compacted using a poker vibrator. The wall elements were cured for two weeks wrapped in plastic in the production hall and subsequently exposed to natural carbonation at a field station (Voll) in a rural area in Trondheim, Norway. An arrangement was prepared to expose the same wall element to both XC3 (moderate humidity, sheltered), and XC4 (cyclic wet and dry, unsheltered) according to EN 1992 [14], as shown in Fig. 2, right.

The average temperature, relative humidity, and CO₂ concentration during the exposure period are given in Fig. 3. The wall elements are kept allowing for future long-term data.

2.2. Methods

2.2.1. Laboratory specimens

2.2.1.1. Carbonation. Carbonation was detected by spraying thymolphthalein solution (1% in mass) on a freshly split surface. Eight series of measurements were performed during the five-year exposure time.

The distribution of the carbonation depth was determined in the plain specimens by image analysis using a colour threshold principle and using the procedure described by Revert et al. [15]. The measurements were performed on all sides, about 40 measuring points per side (3/cm). Aggregates were avoided. The carbonation depth was measured after the preconditioning, and during the exposure period.

The degree of carbonation of the steel-concrete interface (considering the exposed/non-waxed part only) was quantified on the reinforced specimens using the procedure described by Revert et al. [15]. Each specimen was cut in six pieces, each with one reinforcement bar. The pieces were longitudinally split, and the reinforcement was carefully removed to preserve the reinforcement imprint. The imprint was sprayed with thymolphthalein and the degree of carbonation of the

steel-concrete interface determined: The steel-concrete interface was discretized in 1 × 1 mm grid using an image analysis software (Image J). The colour change of the pH-indicator was assessed using a colour threshold principle on each cell (carbonated or non-carbonated). The degree of carbonation is given in a scale ranging from 0 (not carbonated) to 1 (fully carbonated).

2.2.1.2. Open circuit potential. The open circuit potential (OCP) of the embedded steel was measured using the embedded reference electrode and a high-impedance voltmeter. An external saturated calomel (SCE) or copper/copper sulfate (Cu/CuSO₄) reference electrode were used to verify the stability of the embedded reference electrodes. Ultrasound gel was applied on the concrete surface to provide electrical contact between the specimen and the external electrode. To allow comparison of OCP data, all values are given with reference to the copper/copper sulfate (Cu/CuSO₄) electrode. Six series of measurements were performed during the five-year exposure time.

2.2.1.3. Corrosion rate. The corrosion rate of the reinforcement was determined using linear polarization resistance (LPR). A potentiostat PARSTAT 2273 with three-electrode set up was used: embedded reference electrode ERE 20, a titanium mesh applied to the concrete surface as counter electrode, and the reinforcement as working electrode. The embedded counter electrodes did not allow to sustain stable electrochemical measurements and an external titanium mesh was used instead. The reinforcement was polarized ±10 mV from the OCP at a rate of 0.167 mV/min as recommended e.g. by Andrade et. al. [16]. The ohmic drop between the reference electrode and working electrode was determined using AC electrochemical impedance spectroscopy applying an alternating sinusoidal voltage of 10 mV in the range of 500 kHz to 1 Hz. The ohmic drop was determined as the value with the lowest phase angle. The corrosion rate was calculated using the Stern-Geary equation [17] assuming B=26 mV [16]. The exposed area (area not covered by wax) of the reinforcement was used to determine the “(measured) corrosion rate”. Three series of measurements were performed during the five-year exposure time.

2.2.1.4. Electrical resistivity. The electrical resistivity of the concrete was determined using an LCR meter between each couple of neighbouring carbon steel bars. As the distance between bars (40 mm) is more than double of the cover depth (20 mm) the measured resistivity will include both the carbonated cover concrete and the non-carbonated bulk concrete. The frequency was adjusted to find the lowest phase angle. The cell constant of the arrangement was determined in a solution of known resistivity before casting the specimens. Three series of measurements were performed during the five-year exposure time.

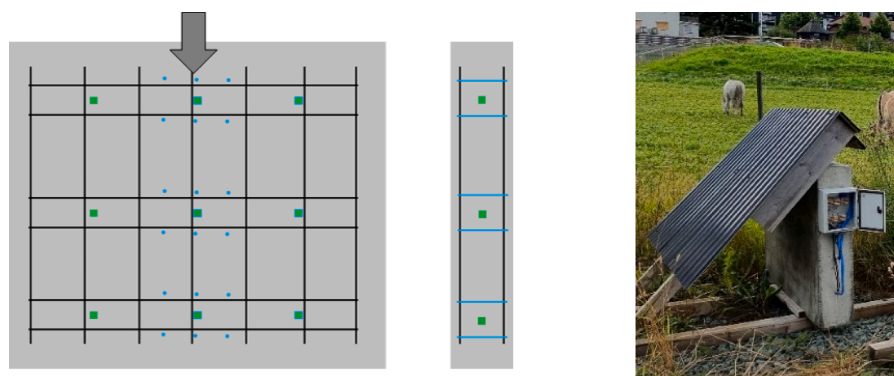


Fig. 2. Left: Sketches of reinforcement and sensors in the instrumented reinforced field exposed wall elements (1500 × 1300 × 250 mm). Reinforcement is presented in black, resistivity probes in blue, and reference electrodes in green. The arrow from the top shows the casting direction. Right: Photo of field exposure station at Voll, Trondheim, Norway. Arrangement to provide one-sided shelter of wall elements, where one side is exposed to XC3 (sheltered), and the other side to XC4 (unsheltered) according to EN 1992.

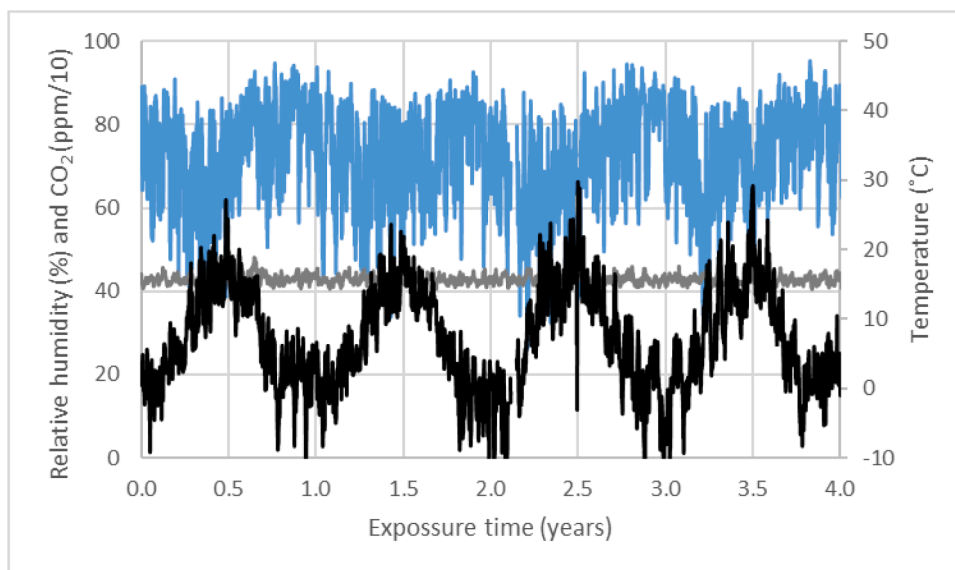


Fig. 3. Field exposure conditions (data gathered from the nearest wear station) during the first four years of exposure (from January 2016 to January 2020). Blue, relative humidity (%), and grey CO_2 concentration (ppm) are presented in the same axes (CO_2 is multiplied by a factor of 0.1), and temperature ($^{\circ}\text{C}$) is presented in the other axes in black.

2.2.2. Field specimens

2.2.2.1. Carbonation. Carbonation of the field exposed wall elements was determined on drilled cores 75 mm in diameter taken from the non-reinforced wall elements. A core included a side exposed to XC3 and a side exposed to XC4. The cores were longitudinally split, and seven measuring points were taken on each of the two exposed end surfaces (1 measuring point/cm, avoiding aggregates).

Two series of measurements were performed during the six-year exposure time.

2.2.2.2. Open circuit potential. The open circuit potential (OCP) of the embedded steel was measured using the embedded reference electrode and a high-impedance voltmeter. An external copper/copper sulfate (Cu/CuSO_4) was used to verify the stability of the embedded reference electrodes. Ultrasound gel was applied on the concrete surface to provide electrical contact between the specimen and the external electrode.

Four series of measurements were performed during the six-year exposure time.

2.2.2.3. Electrical resistivity. The electrical resistivity of the concrete was determined using an LCR meter between each couple of neighbouring resistivity probes. The resistivity probes were mounted between bars in the middle of the cross section of the field specimens, thus it is expected that this measurement gives a measure of the bulk resistivity of the concrete (non-carbonated). The frequency was adjusted to find the lowest phase angle. The cell constant of the arrangement was determined in a solution of known resistivity before casting the wall elements. Four series of measurements were performed during the six-year exposure time. To limit the potential effect of seasonal variations in moisture and temperature, the field measurements were undertaken at the same time of the year and comparable exposure conditions.

4. Results

4.1. Carbonation of unreinforced laboratory exposed specimens

Comparable carbonation distributions were measured on all the sides (bottom, top, and lateral) of the unreinforced specimens, and the data is therefore not differentiated.

Fig. 4 presents the carbonation development in the unreinforced laboratory specimens using box and whisker diagrams. The whiskers show the maximum and minimum values while the boxes show the median, first, and third quartile of the carbonation distributions. Note that the horizontal axes indicate the exposure time but scaled according to number of measuring points. Outliers smaller/greater than 1.5 times the interquartile range were omitted (only one point was omitted).

Table 3 presents the coefficient of variation (CoV) of the carbonation depth distributions in the unreinforced laboratory specimens over time. The CoV was in the same range for all the specimens, but slightly lower for FA-specimens.

The carbonation depth distributions in the unreinforced laboratory specimens after ca. five years of exposure (250 weeks) are given in **Fig. 5**. The depth of carbonation was higher in the FA specimens, and largest for the concrete with 30% FA.

4.2. Reinforced laboratory exposed specimens

Photos of the reinforced specimens after the longitudinal cutting before extracting the reinforcement, after spraying with thymolphthalein, and of the reinforcement bars are given in **Appendix A**.

Table 4 presents the degree of carbonation (DoC) of the concrete-steel interface, and the estimated corroded area (CA) of the reinforcement after five years of laboratory exposure. The estimated corroded area is given for the outer and the inner side of the reinforcement in relation to the exposed concrete surface.

Fig. 6 presents the development of the average open circuit potential (OCP), the electrical resistivity and the corrosion rate during the five years exposure period. After initial stabilisation, the OCP became more negative over time, as expected. The potential drop from the start of the experiments to the end of the five year's exposure period varied depending on the cement type. The resistivity measurements show an increase in the electrical resistivity over time for all the specimens, especially for the fly ash blends. Similar corrosion rate trends were observed for all the specimens. Slightly higher corrosion rate values (and higher scatter) were measured on the 30% FA specimen.

Fig. 7 presents the measured degree of carbonation of the steel-concrete interface, the measured corrosion rate, the OCP, and the electrical resistivity after five years laboratory exposure. The fly ash containing concretes (18% FA and 30% FA) had comparable average degree

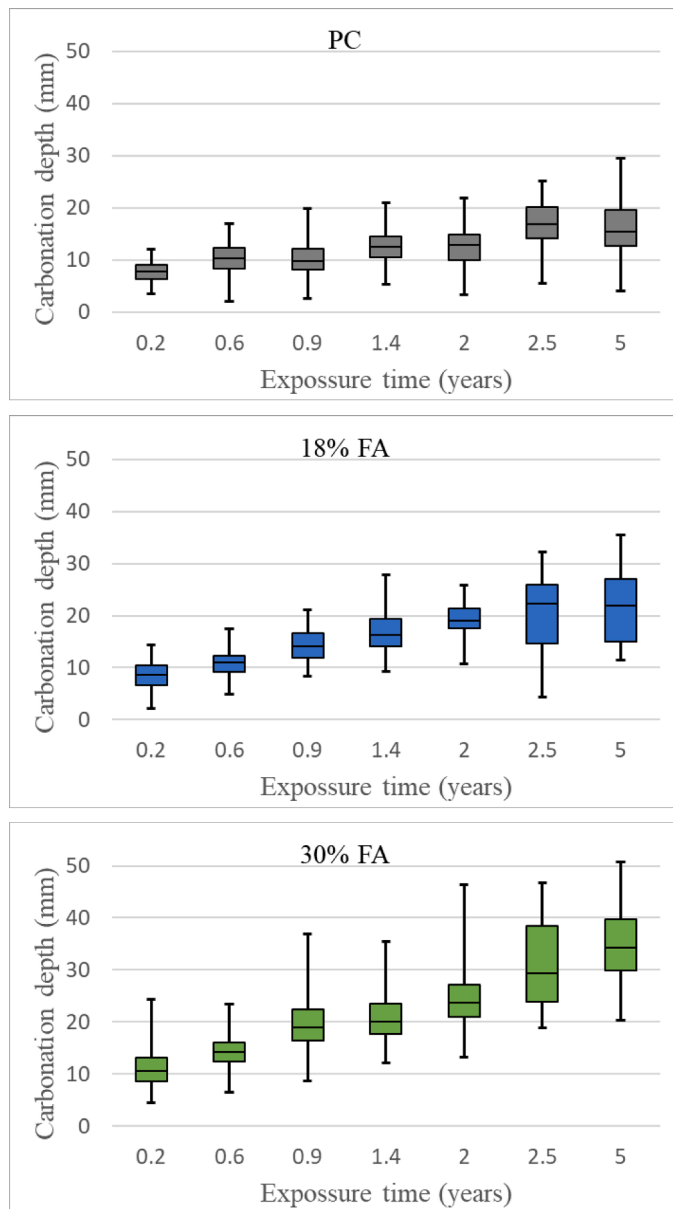


Fig. 4. Box and whisker diagram showing carbonation development over the exposure period of five years in unreinforced concrete specimens with and without fly ash in laboratory exposure. The whiskers show the maximum and minimum values while the boxes show the median, and the first and third quartile of the carbonation distributions. PC (grey), 18% FA (blue), and 30% FA (green).

Table 3
Coefficient of variation (CoV) over of the exposure time, unreinforced laboratory specimens

Exposure time (years)	0.2	0.6	0.9	1.4	2.0	2.5	5
PC	24	27	32	24	32	25	34
18% FA	28	20	22	25	17	33	22
30% FA	29	22	28	21	24	26	19

of carbonation and higher degree of carbonation compared to the concrete without fly ash (PC). The OCP of the PC concrete presented positive values (20-120 mV), while the 18% FA concrete showed OCP in the range ± 100 mV. The 30% FA concrete showed less variation between bars and a lower OCP with an average value of -280 mV. The scatter on the resistivity measurements is limited, also between top and bottom

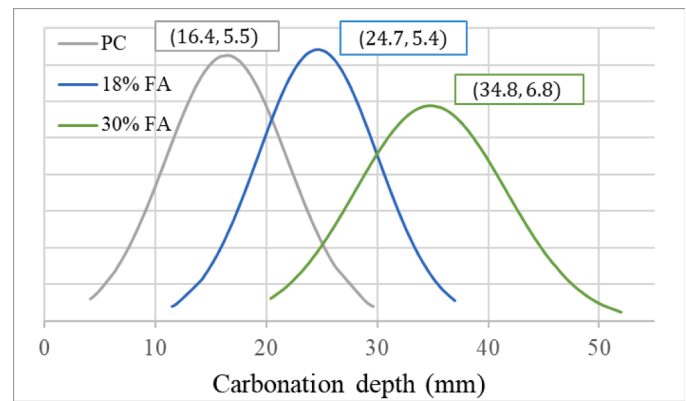


Fig. 5. Carbonation depth distributions after five years of laboratory exposure measured on unreinforced specimens. Average value and standard deviation (STD) are given in the figure as [average, STD].

Table 4
Degree of carbonation (DoC) and corroded area (CA) after five years of laboratory exposure. The estimated corroded area is given for the outer and inner side of the reinforcement.

Bar #	PC			18% FA			30% FA		
	DoC (%)	CA (%)		DoC (%)	CA (%)		DoC (%)	CA (%)	
		Out	In		Out	In		Out	In
1	60	<10	0	80	<10	0	90	>90	>10
2	50	<5	0	85	<20	0	80	>80	<10
3	40	0	0	70	<10	0	95	>70	>20
4	80	0	0	90	<10	<10	99	<30	<50
5	95	0	0	95	0	0	90	<40	<30
6	70	0	0	99	<10	<10	95	<50	<20

bars. The average values are approximately 360 $\Omega \bullet m$ for the concrete without fly ash (PC), 1200 $\Omega \bullet m$ for the concrete with 18% FA, and 1500 $\Omega \bullet m$ for the concrete with 30% FA. The measured corrosion rate after five years of exposure presented some variation, within the same specimen regardless the bar position (top or bottom).

4.3. Field exposed specimens

Table 5 presents the carbonation development during the exposure period. Lower carbonation development was observed in general in the XC4 (unsheltered) condition compared to XC3 (sheltered). As expected, lower carbonation resistance was found for the fly ash blends. None of the concretes were carbonated to the depth of the reinforcement.

Fig. 8 presents the electrical resistivity during the exposure period. The resistivity measurements show an increase in the electrical resistivity over time for all the specimens, especially for the fly ash blends. Following conditions were reported for the resistivity measurements (T, RH): First measurement (20 °C, 51%), second (20 °C, 51%), third (13 °C, 62%), and fourth and final (17 °C, 55%). It should be noted that the resistivity probes were mounted in the middle of the cross section of the field exposed wall elements and thus give a measure of the resistivity of the bulk concrete which is presently not carbonated. In addition, variation in moisture and temperature of the concrete will influence the measured values.

Table 6 presents the OCP of the reinforcement bars in the field exposed wall elements after six years, in exposure class XC3 and XC4. OCP measured against an external copper/copper sulphate electrode after six years of exposure showed lower OCP on the XC4 exposure condition compared to XC3. The OCP varied within the concretes.

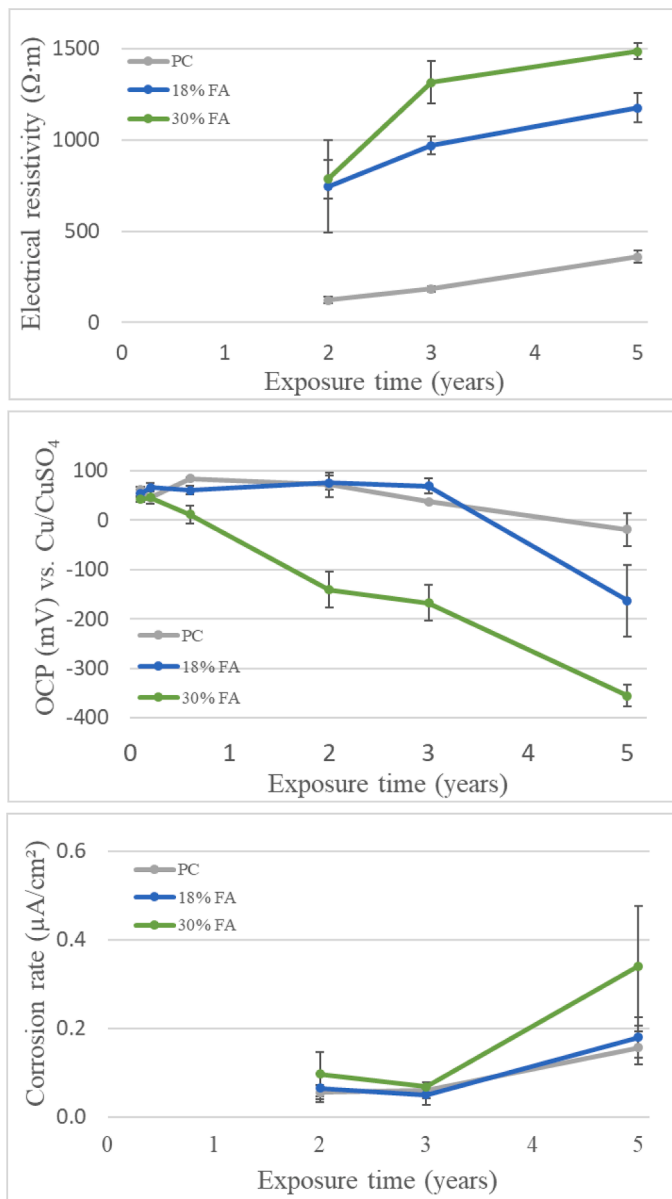


Fig. 6. Development of, electrical resistivity, open circuit potential and corrosion rate in the reinforced specimens during five years of laboratory exposure; PC (grey), 18% FA (blue), and 30% FA (green). Average and range indicated.

5. Discussion

In an earlier study, the carbonation products of the investigated cements after carbonation at different laboratory conditions (a) 60% RH and 1% CO₂, b) 90% RH and 5% CO₂ and c) 60% RH and 100% CO₂ and at natural conditions were compared [18]. The combined observations on microstructure and phase assemblage indicated that carbonation up to 5% CO₂ is representative for natural carbonation [18]. Pore solution analysis revealed similar trends for the three accelerated carbonation conditions, whereas pore solution data for the naturally exposed specimens were non-conclusive due to limited carbonation [11]. Based on the observations of carbonation at 90% RH and 5% CO₂ being representative for natural carbonation regarding microstructure and phase assemblage, and assuming a similar phase assemblage results in a similar pore solution composition, the findings suggest that for the investigated binders, the accelerated carbonation condition used for the present investigation (90% RH, 5% CO₂) might be used for corrosion rate

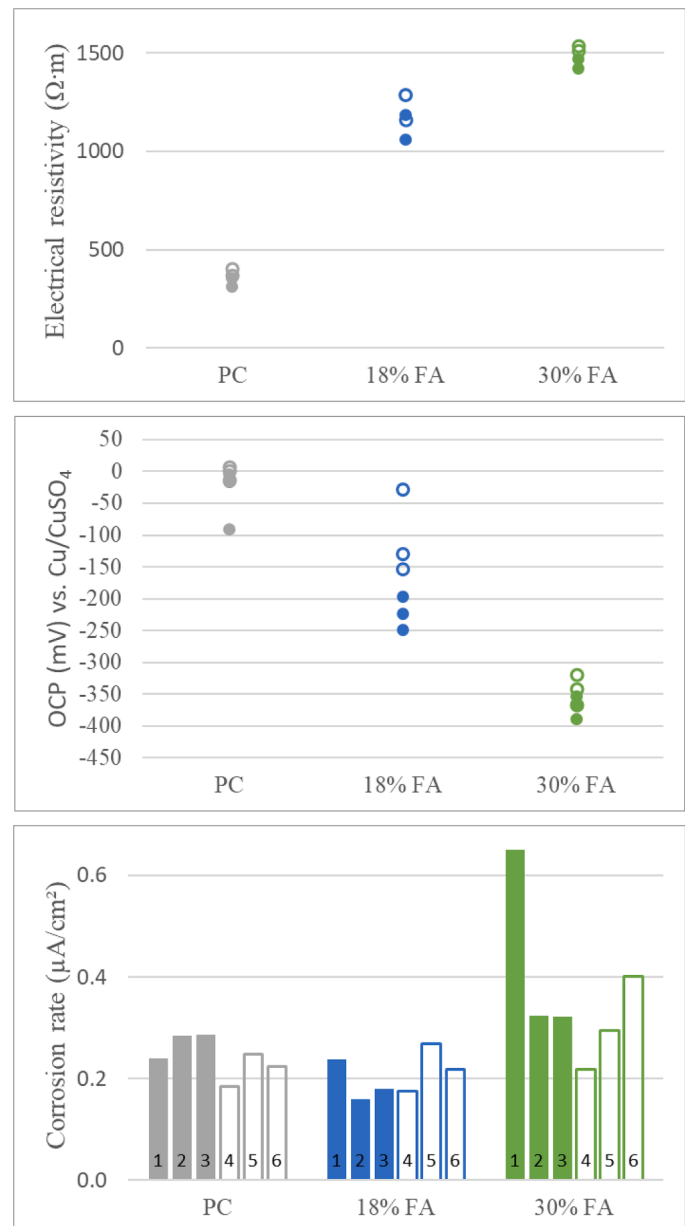


Fig. 7. Electrical resistivity, open circuit potential (OCP), and corrosion rate measured in reinforced specimens after five years of laboratory exposure; PC (grey), 18% FA (blue), and 30% FA (green). Bottom bars (solid symbols), top bars (open symbols.)

Table 5

Carbonation development in the field exposure wall elements (average, mm)

	PC		18% FA		30% FA	
	1 year	6 years	1 year	6 years	1 year	6 years
XC3	2.8	9.3	3.8	9.7	4.1	13.9
XC4	3.3	7.4	4.1	8.5	4.9	9.7

studies.

5.1. Carbonation development

From Table 3 it can be observed that the coefficient of variations (CoV) of the carbonation depth appears neither binder nor time dependent in the laboratory exposed specimens. Table 7 summarises the

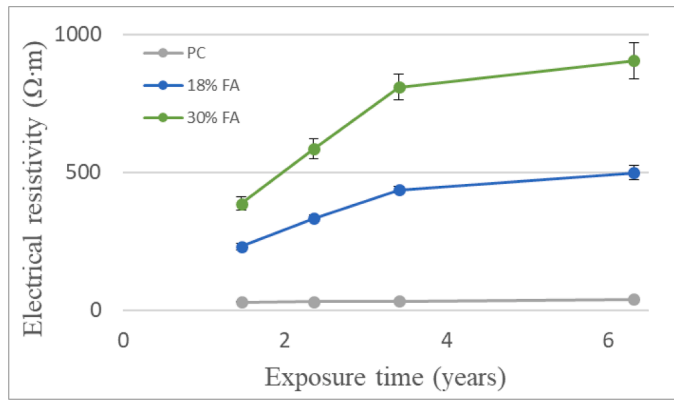


Fig. 8. Electrical resistivity development during six years of field exposure. PC (grey), 18% FA (blue), and 30% FA (green).

Table 6

Open circuit potential (OCP) of the reinforcement bars in the field exposure wall elements after six years in exposure class XC3 (sheltered) and XC4 (unsheltered), average values vs Cu/CuSO₄. Each wall element contains six electrically isolated horizontal reinforcement bars on each side (#1-6 from bottom to top).

Bar #	OCP (mV) vs. Cu/CuSO ₄					
	PC		18% FA		30% FA	
	XC3	XC4	XC3	XC4	XC3	XC4
6	73	-32	15	-20	156	25
5	80	-30	-5.2	-45	86	-44
4	60	-40	187	-87	158	35
3	20	-89	227	-77	60	1
2	-64	-45	-3	-20	6	-89
1	32	-56	-1	-41	1	-89

carbonation depths measured in the unreinforced laboratory specimens and the field exposed wall elements after five and six years, respectively. The CoV of the carbonation depth of the laboratory exposure varied between 19% and 34%. For the field exposed wall elements, the CoV was lower for the 30% FA in both exposure conditions (11-13%), while PC and 18% FA presented values between 17% and 29%.

The same ranging of the three investigated cements with regard to carbonation resistance was obtained in laboratory and field exposure (see Table 4). But the relative performance of the fly ash blends was poorer in accelerated carbonation compared to the field performance, especially for the 30% FA. The field data showed comparable carbonation performance for the PC and 18% FA, especially when exposed to XC3. Similar observations were registered by Leemann and Moro [19], who tested different concretes at 57% RH and 1% CO₂, 80% RH and 4% CO₂, and in the field at XC3 and XC4. Comparable carbonation performance was observed for XC3 and 57% RH, while the relative carbonation resistance differed at 80% RH and XC4. They attributed this feature to the capillary condensation, which becomes of increased importance at higher moisture levels. For lower humidities the carbonation resistance is governed by the CO₂ buffer capacity [19].

Table 7

Carbonation depth (average, relative average and CoV) measured in the unreinforced laboratory specimens and field exposed wall elements after five and six years, respectively.

	Laboratory (after 5 y)			Field (after 6 y)					
	Ave (mm)	STD (-)	CoV (%)	XC3			XC4		
				Ave (mm)	STD (-)	CoV (%)	Ave (mm)	STD (-)	CoV (%)
PC	16.4	1	34	9.3	1	17	7.4	1	26
18% FA	24.7	1.5	22	9.7	1	29	8.5	1.2	26
30% FA	34.8	2.1	19	13.9	1.5	11	9.7	1.3	13

Fig. 9 presents the carbonation development over time in the laboratory exposure (note that square-root time is used for the horizontal axes). For all three concretes, the carbonation rate showed square-root time dependency the first 2.5 years. The fitting was performed using data from 0.2 to 2.5 years and allowing a potential initial offset. This was done despite no carbonation was observed on the sealed cured laboratory specimens. This is done in order to avoid the influence of a potential faster early carbonation development, which is a challenge when testing carbonation, especially on blended cements. The last measurement (after five years) showed a deviation from the previous trend (up to 2.5 years), indicating reduced long-term carbonation rate for all three binders. The long-term less than square-root time dependency could be explained by the formation of carbonates at the outer surface of particles reducing the further carbonation rate. Studies of the carbonation front in mortars made from the same cements showed potentially a gradual reduction in calcium hydroxide and formation of calcium carbonate, but also method dependent observations [20]. A broader width of the carbonation front was observed with thermogravimetric analysis (TGA) than with optical microscopy and pH indicator, which was partly explained by the impact of sampling (ground samples from a given depth range being used for TGA) [20].

5.2. Carbonation distribution in reinforced laboratory exposed specimens

The measured degree of carbonation of the steel-concrete interface varied depending on the cement and the position of the bars (Table 4). The highest degree of carbonation of the steel-concrete interface was observed for top-bars and for the FA concretes.

For comparison of unreinforced and reinforced specimens, the degree of carbonation of the steel-concrete interface was estimated from the carbonation depth distribution determined on the unreinforced specimens (Fig. 5) considering the position of the reinforcement (concrete cover 20 mm, bar diameter 16 mm), see table Table 8. The

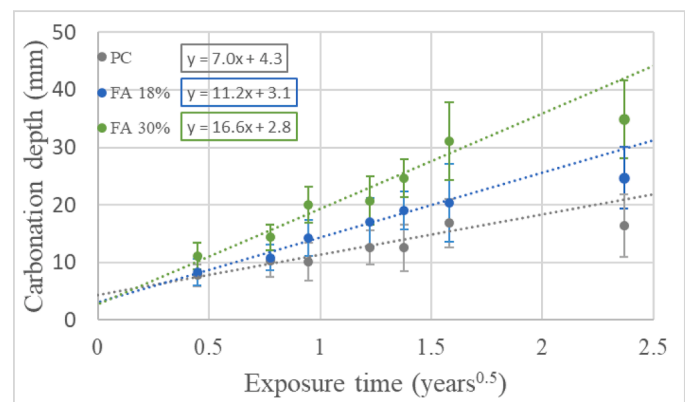


Fig. 9. Carbonation development over five years of laboratory exposure measured on unreinforced specimens. Average value and standard deviation are indicated in the figure. Note that square-root scale is used on the horizontal axes. The dotted lines represent the best-fit of the raw data from ca. 0.2 to 2.5 years of exposure.

Table 8

Comparison of the measured and estimated degree of carbonation of the steel-concrete interface. The degree of carbonation was estimated based on the carbonation depth distributions in the unreinforced specimens.

	Estimated degree of carbonation (based on unreinforced specimens)	Measured degree of carbonation of the steel concrete interface
PC	0.3	0.7
18% FA	0.8	0.9
30% FA	1	0.9

measured degree of carbonation is for the PC much higher than that estimated from the unreinforced specimen, whereas they are in the same range for the FA concretes. The latter could be explained by the relatively large carbonation depths already achieved for the reinforced FA concrete.

Fig. 10 further illustrates the observations made for the PC specimens. The unreinforced specimen presented a carbonation distribution after five years of exposure of 16.4 mm on average (Fig. 6), which gives a predicted degree of carbonation of the steel concrete interface of ca. 0.3 (Table 5). The reinforced specimen presented deeper carbonation depths around the reinforcement (measured degree of carbonation 0.7).

The feature of increased carbonation depth at the steel-concrete interface as well as the impact of the bar position was previously observed on reinforced mortar specimens made from the same cements and suggested explained by microstructural defects in the vicinity of the reinforcement [15]. These observations were used to explain the apparent early onset of corrosion reported in the literature when comparing carbonation depth data from unreinforced specimens with corrosion measurements on reinforced specimens [15]. Observations of increased carbonation depth in the vicinity of the reinforced has also been reported [21]. This feature is a challenge for service life design and reassessment of concrete structures undergoing carbonation. In relation to chloride induced corrosion, an increased awareness has been created for the potential role of the local characteristics of concrete-steel interface for the carbonation of the interface, as well as for the initiation and propagation of corrosion [22].

5.3. Corrosion development

No data on corrosion rate is yet available from the field exposed wall elements and the below discussion is solely based on the laboratory specimens.

Both the cement type and the bar positions were found to affect the corrosion development in the laboratory exposed specimens. The

corroded area is substantially higher on bars extracted from the 30% FA concrete than on bars from the 18% FA and the PC concretes (Table 4). This might either be explained by an earlier corrosion initiation in the 30% FA concrete, as reflected in the OCP development (see Fig. 6) or an actual higher corrosion rate. Earlier studies of the pore solution composition in carbonated mortars made from the PC and the 30% FA cement showed similar measured free Na, K, S and Cl contents, whereas calculations of the pH indicated slightly lower values in the 30% FA mortar than in PC, 9.7 vs 10.9 [11]. De Weerd et al. discussed the impact of the changes in pore solution composition during carbonation and found that the typically used $[\text{Cl}^-]/[\text{OH}^-]$ and $[\text{SO}_4^{2-}]/[\text{OH}^-]$ thresholds would be reached before complete carbonation. The $[\text{Cl}^-]/[\text{OH}^-]$ and $[\text{SO}_4^{2-}]/[\text{OH}^-]$ were in the range of 100 for the PC mortar and in the range of 1000 for the 30% FA mortar, both in carbonated condition [11].

In addition to the cement type, also the position of the bars was found to affect the corrosion development. Larger corroded areas were observed on bottom bars than on top bars for all three types of cement, and in the case of PC and 18% FA corrosion was only observed on bottom bars (#1-3) (Table 4). The visual observation of corroded area is, especially for the 18% FA concrete, in agreement with the slightly lower OCP values measured for the bottom bars whereas limited differences in corrosion rate of bottom and top bars were measured (see Appendix A).

Comparing the measured degree of carbonation of the steel-concrete interface and the corroded area, the impact of cement type is reflected in both parameters, whereas despite a lower degree of carbonation of the steel concrete interface a larger corroded area is observed for bottom bars than for top bars. A potential explanation might be a difference in microstructure and porosity causing a higher moisture retention at the bottom bars at the laboratory conditions used (90% RH, 20°C). A companion study revealed a position dependent microstructure in the vicinity of steel bars in mortar specimens [15].

A decreased OCP is observed for increasing degree of carbonation see Fig. 11. The correlation between the parameters appears to be cement and bar position dependent. Slightly lower OCP is observed for bottom bars, despite higher degree of carbonation of top bars. The largest impact appears to be the binder. The largest OCP drop (about 400 mV) is observed for the 30% FA specimen, while the average OCP drop for the 18% FA and the PC specimens were in the range of 200 and 100 mV respectively. In a previous investigation a relationship was found for reinforced mortar specimens prepared with 30% FA carbonated and stored at 1% CO_2 and 60% RH, with OCP of 100 mV in non-carbonated condition to -100 mV in carbonated condition [15].

The measured corrosion rates in the current investigation are in the range of reported corrosion rates at 90% RH [7,8]. When comparing to a recent study [9], the corrosion rates in the current investigation are

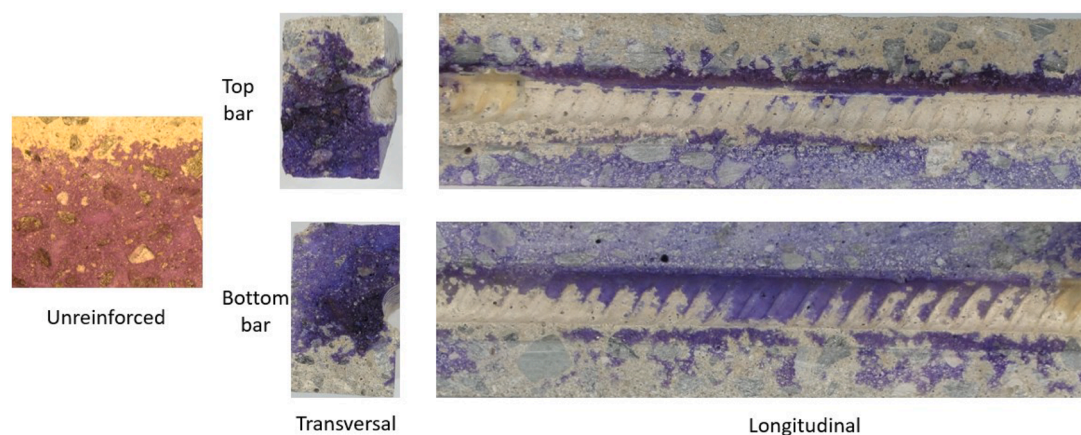


Fig. 10. Comparison of carbonation depth distribution after five years in the unreinforced (left) and the reinforced laboratory exposed PC specimens. Imprints of (bar #2 and #5) transversal (middle) and longitudinal reinforcement (right). The difference in color is due to different light setting.

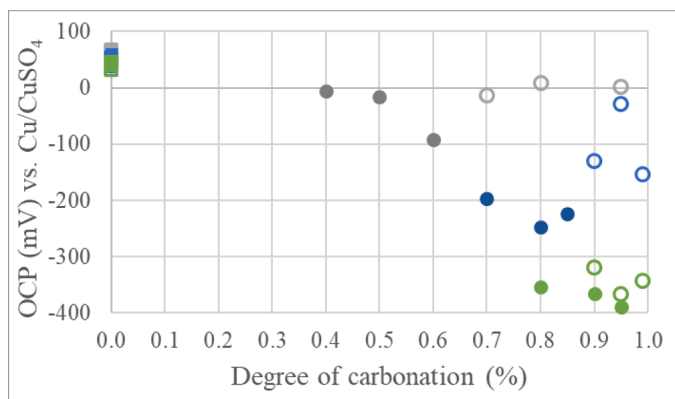


Fig. 11. Correlation between the degree of carbonation and the OCP: at the initiation of the exposure (degree of carbonation 0), and after five years of exposure in the reinforced laboratory exposed specimens; PC (grey), 18% FA (blue), and 30% FA (green). 1-3 bottom bars (solid symbols), 4-6 top bars (open symbols)

about one order of magnitude higher for the PC, and about five times higher for the FA at 90% RH. The concrete recipe and preconditioning might have an influence on the differing results. Furthermore, it is not known if the corrosion rates were compensated for the ohmic drop in [9]. This will lead to lower corrosion rate.

It seems that the so-called top-bar effect [23] had a limited influence on the carbonation of the steel-concrete interface and the propagation of corrosion. Comparable values were measured for top and bottom bars within each specimen. It should be noted that the difference in height between top and bottom bars is limited (about 65 mm between centre of the reinforcement).

It should be mentioned that this investigation only considers corrosion activity of isolated reinforcement bars. In concrete structures the reinforcement bars are in contact with other bars which can lay in (partly) carbonated concrete. This might lead to microcell corrosion [24].

5.4. Guidelines

Guidelines for assessment of the corrosion level based on electrical resistivity and corrosion rate according to [25] and OCP according to [26,27] are compared to the measured values from the corroding reinforcement in the laboratory exposed specimens and summarized in Table 9. It can be observed that the assessment of the risk of corrosion depends on the parameter used for the evaluation; even for the PC concrete for which most experience is available.

Table 9

Guidelines for assessment of the corrosion level based on electrical resistivity and corrosion rate according to [25] or OCP according to [26,27] and measured values.

	Corrosion level	Resistivity	Icorr	Vcorr	Corrosion level	OCP vs SCE
		(Ω m)	(μA/cm ²)	(μm/y)		(mV)
Guidelines	Negligible	> 1000	≤ 0.1	≤ 1	Passivity	> -200
	Low	500 to 1000	0.1 to 0.5	1 to 5	General	-200 to -350
	Moderate	100 to 500	0.5 to 1	5 to 10		-350 to -500
	High	<100	>1	>10	-	< -500
Laboratory exposed specimens	PC	300 to 400	0.2	2	0 to 10	-20 to 80
	18% FA	1000 to 1300	0.2	2	0 to 30	-200 to 50
	30% FA	1500	0.2 to 0.6	2 to 6	<30 to >70	-320 to -240

The OCP values registered in the PC specimen were higher than those for passivity in aerated concrete according to [26], while the 18% FA specimen had values representative for passivity in aerated concrete, and the 30% FA specimen was in the range for general corrosion in carbonated concrete. Similar ranging, but more severe assessment is obtained if considering the measured corrosion rate, which according to [25] is classified as low for the PC and 18% FA, and low to moderate for the 30% FA. In contrast, the risk of corrosion based on the concrete electrical resistivity is according to [25] assessed negligible for 18% and 30% FA specimens, while moderate for the PC.

The initiation period depends on the carbonation of the steel-concrete interface, but also on whether active corrosion initiates, which is highly moisture dependent and indeed not always the case [22]. The duration of the propagation period depends on the corrosion rate as well as the extent of corrosion causing the limit state, e.g., cracking, to be surpassed. A typical value used for the durability limit state is a cross sectional reduction of 50 μm [28], which for the investigated concretes in laboratory condition (90% RH and 20C), and based on the measured values is estimated to take place between 10 and 25 years after corrosion initiation; shortest for the 30% FA concrete and longest for the PC and 18% FA.

The present investigation of concrete from cements varying in fly ash content illustrates the need for long-term data and further understanding of the actual mechanisms and controlling factors of both the process of carbonation and the initiation, and propagation of corrosion in carbonated concrete. In the present study it was found that the OCP drop upon carbonation was binder dependant, see Fig. 11. This issue, which is important when assessing corrosion in a structure, is apparently not covered by present guidelines which are based on threshold values.

6. Conclusions

Concretes prepared with plain Portland cement, as well as 18% and 30% FA were exposed to either laboratory conditions at 90% RH, 20°C, and 5% CO₂ for a five-year period or to natural carbonation in a rural area of Trondheim, Norway for a six-year period. Corrosion was only initiated in the laboratory exposed specimens.

The following conclusions are drawn:

1. The rate of carbonation was higher in laboratory exposed specimens than in the field exposed wall elements.
2. The carbonation development in the laboratory specimens showed reduced rate after 2.5 years indicating conservative predictions based on short-term data.
3. An increased carbonation depth was observed at the steel-concrete interface compared to carbonation development in the unreinforced specimens.

4. Comparable corrosion rate was measured for the PC and the 18% FA laboratory exposed concretes, while higher rates were measured for the 30% FA concrete. The difference might be due to an earlier corrosion initiation and a larger fraction of the steel area corroding in the 30% FA at the time of investigation. No field data are yet available for verification of the apparent binder dependent corrosion rates measured on laboratory exposed specimens.
5. Assuming applicable for the laboratory exposed concrete specimens, the assessment of the risk of corrosion varied depending on the parameter used for the evaluation, here electrical resistivity, open circuit potential, and corrosion rate. This questions the general applicability of such guidelines.

Compliance with ethical standards

Information regarding sources of funding are given in the acknowledgments, and potential conflicts of interest (financial or non-financial) are described. Accepted principles of ethical and professional conduct have been followed.

CRediT authorship contribution statement

Andres Belda Revert: Writing – review & editing. **Tobias Danner:**

Appendix A

[Figs. A1, A2, A3, A4, A5, A6, A7, A8, A9](#)

Writing – review & editing. **Mette Rica Geiker:** Writing – review & editing.

Declaration of competing interest

The authors declare no conflicts of interest.

Data availability

The manuscript includes the data.

Acknowledgements

The conceptualisation and initial measurements were part of a larger research project 'Lavkarbsem' (NFR project no. 235211/O30). The project was supported by the Norwegian Research Council and the following companies, Mapei AS, Norbetong AS, Heidelberg Materials Sement Norge AS, Skanska AS, and Rambøll Engineering AS. Their support as well as financial support for finalisation from Norcem AS is greatly acknowledged.

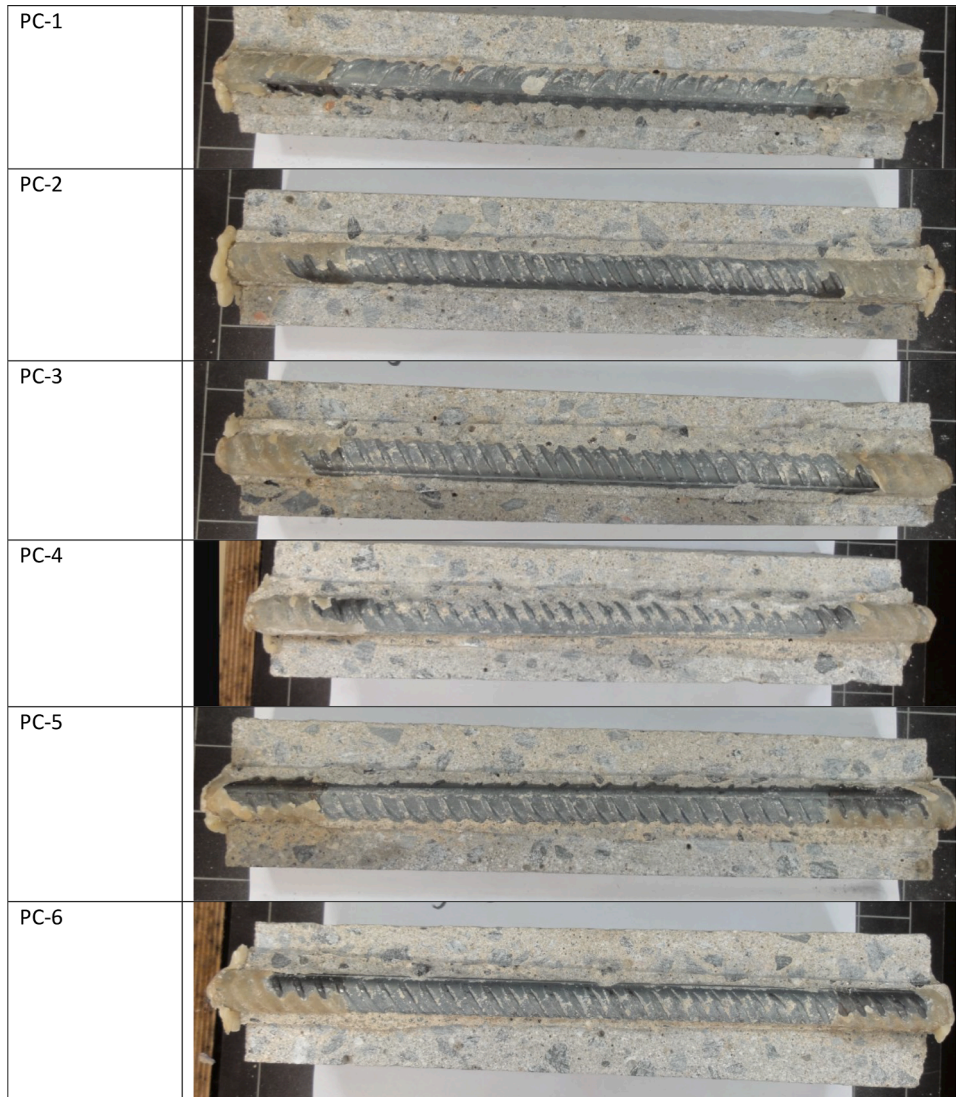


Fig. A1. Longitudinal cut along reinforcement (before removing the reinforcement) of reinforced PC specimen after five years laboratory exposure.

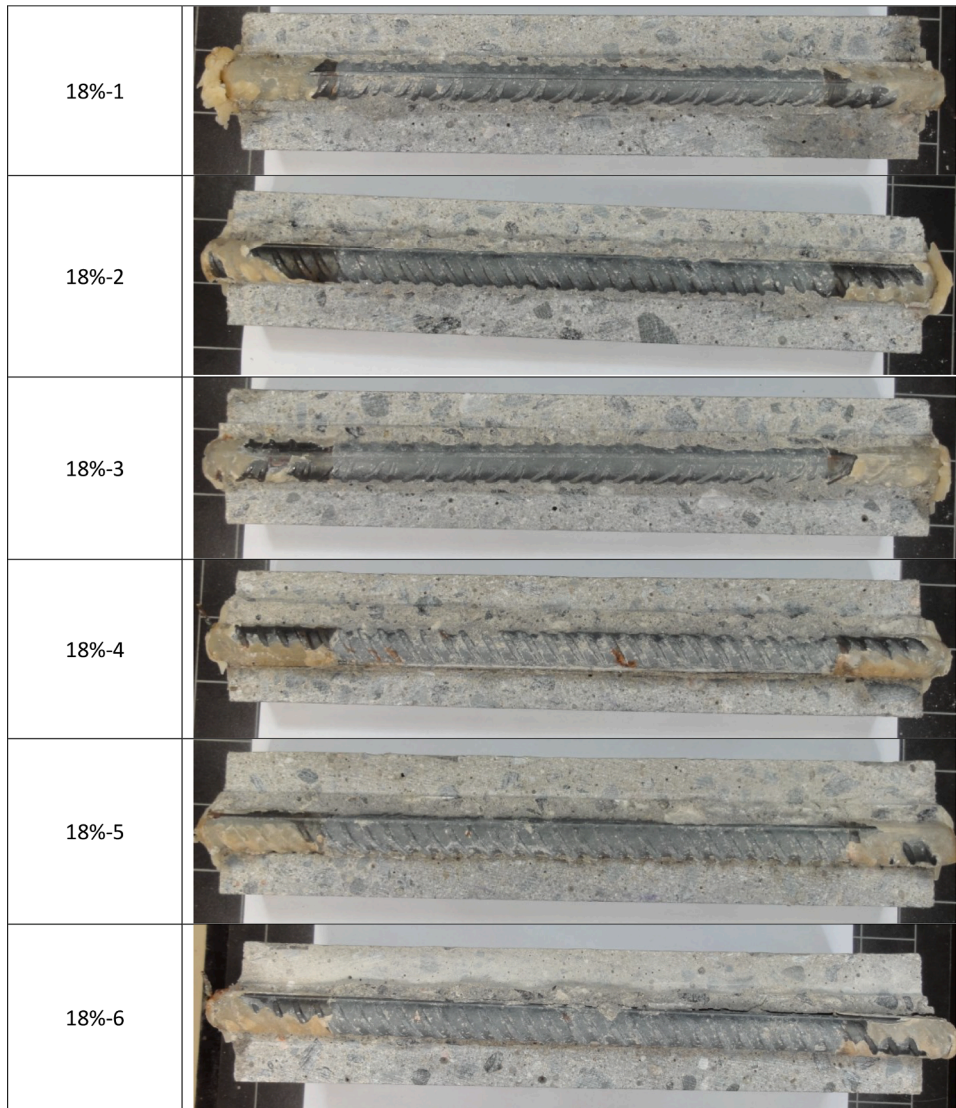


Fig. A2. Longitudinal cut along reinforcement (before removing the reinforcement) of reinforced 18% FA specimen after five years laboratory exposure.

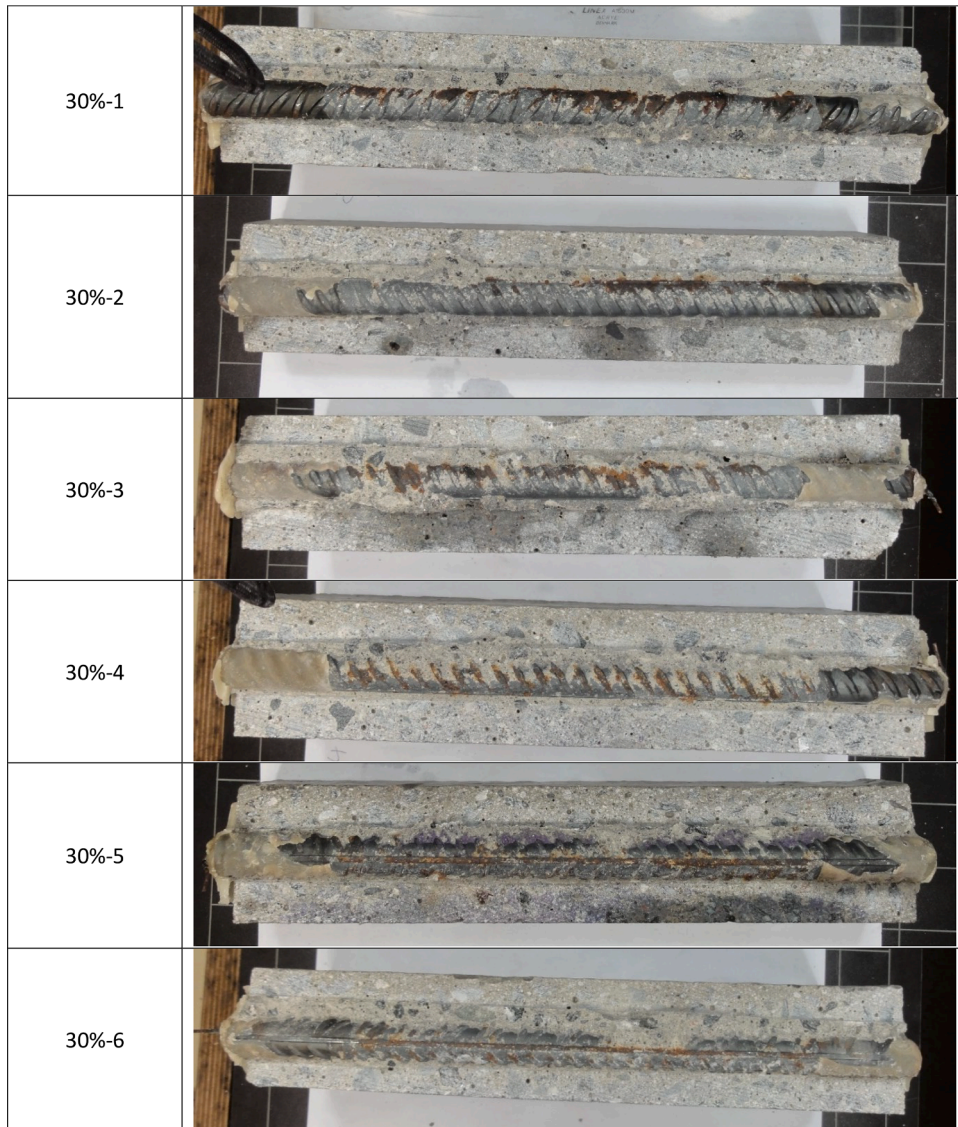


Fig. A3. : Longitudinal cut along reinforcement (before removing the reinforcement) of reinforced 30% FA specimen after five years laboratory exposure.

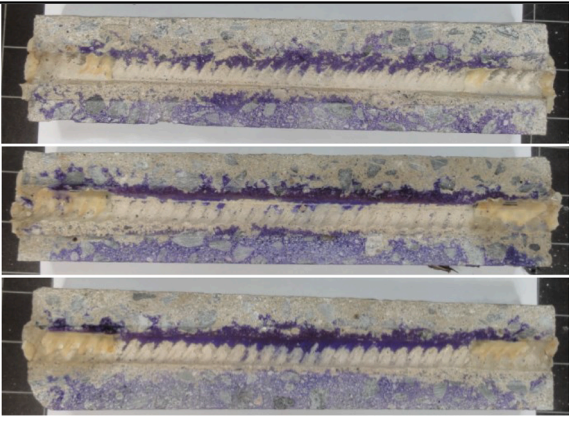
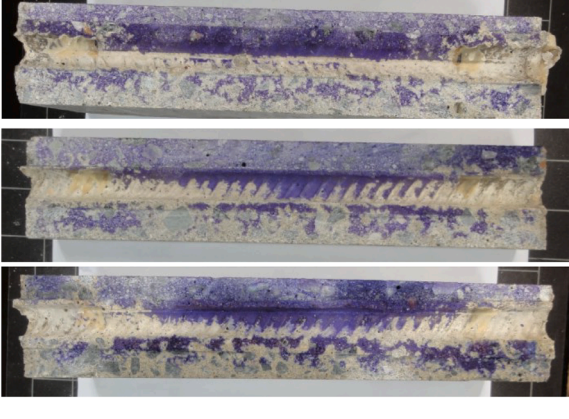
Bars #	Casting direction	Exposure direction	PC
4	↓	↓	
5			
6			
1	↓	↑	
2			
3			

Fig. A4. Steel-concrete interface sprayed with thymolphthalein after five years of reinforced PC specimen after five years laboratory exposure.

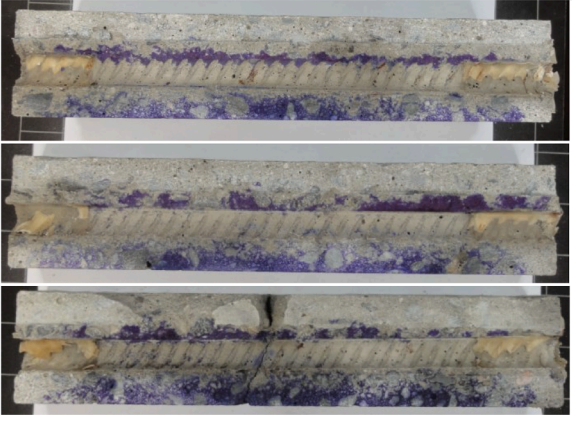
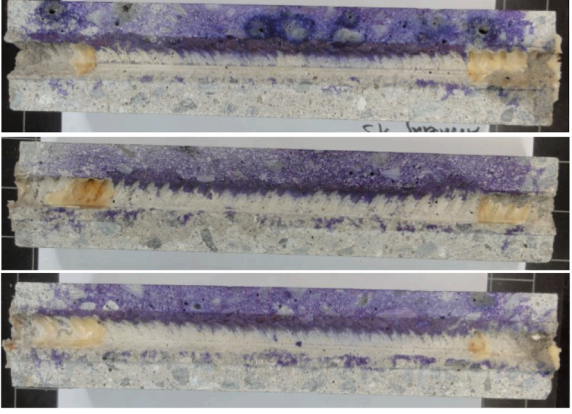
Bars #	Casting direction	Exposure direction	18% FA
4	↓	↓	
5			
6			
1	↓	↑	
2			
3			

Fig. A5. Steel-concrete interface sprayed with thymolphthalein after five years of reinforced 18% FA specimen after five years laboratory exposure.

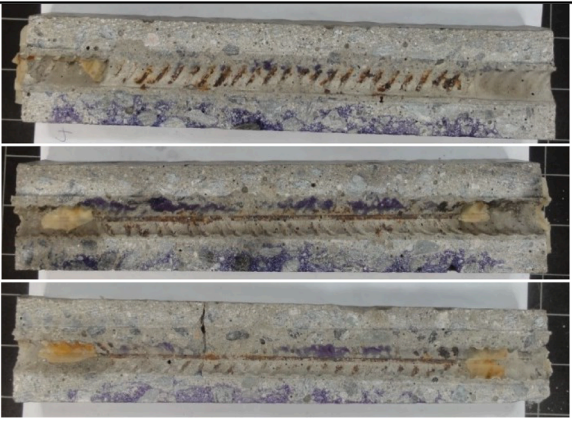
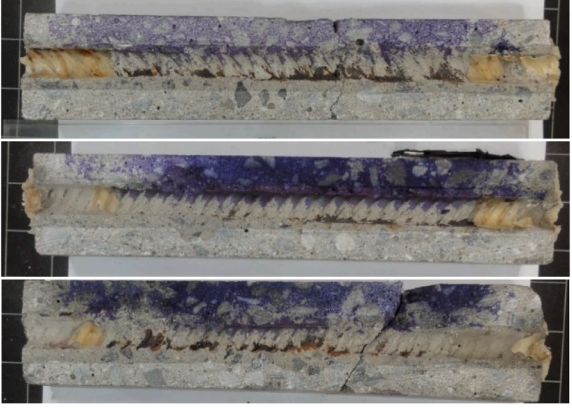
Bars #	Casting direction	Exposure direction	30% FA
4	↓	↓	
5			
6			
1	↓	↑	
2			
3			

Fig. A6. Steel-concrete interface sprayed with thymolphthalein after five years of reinforced 30% FA specimen after five years laboratory exposure.





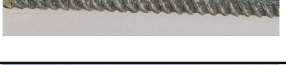
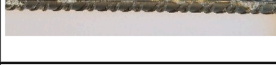





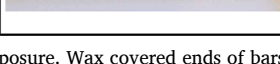
Bars #	PC	
	Inner side	Exposed side
4		
5		
6		
1		
2		
3		

Fig. A7. Reinforcement after removal from PC specimen after five years laboratory exposure. Wax covered ends of bars not shown. 1-3 bottom bars, 4-6 top bars.

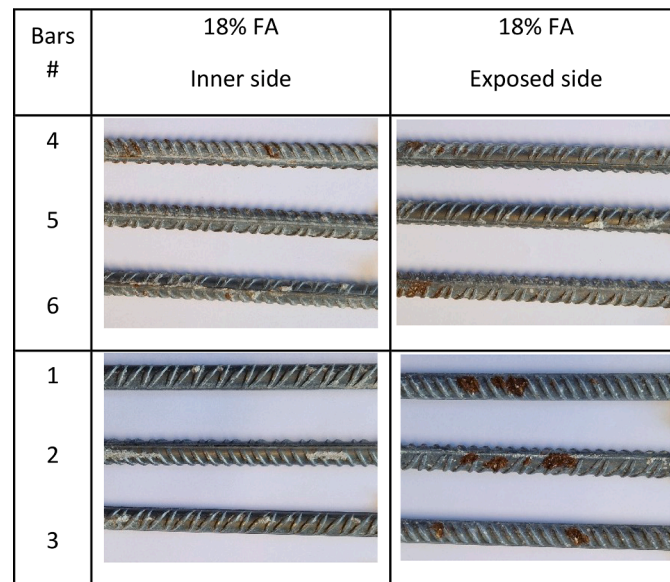


Fig. A8. Reinforcement after removal from 18% FA specimen after five years laboratory exposure. Wax covered ends of bars not shown. 1-3 bottom bars, 4-6 top bars.

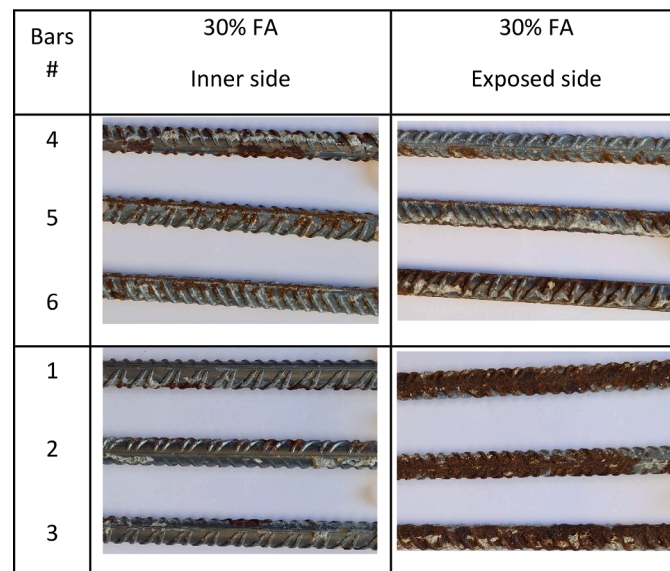


Fig. A9. Reinforcement after removal from 30% FA specimen after five years laboratory exposure. laboratory exposed specimens after five years, Wax covered ends of bars not shown. 1-3 bottom bars, 4-6 top bars.

References

- [1] M. A. Robbie, Global CO₂ emissions from cement production, 1928–2018, Earth System Science Data; Katlenburg-Lindau 11 (Iss. 4) (2019), <https://doi.org/10.5194/essd-11-1675-2019>.
- [2] M. R. Geiker, Fly ash in concrete, Danish experience : State-of-the-art report, Norwegian Road Administration report, 2015. <http://hdl.handle.net/11250/2619249>.
- [3] Personal communication from Steinar Helland.
- [4] fib, International Federation for Structural Concrete, fib, Model Code for Service Life Design, Bulletin no 34, in, Lausanne, Switzerland, 2006.
- [5] U. Angst, F. Moro, M.R. Geiker, et al., Corrosion of Steel in Carbonated Concrete: Mechanisms, Practical Experience, and Research Priorities – a Critical Review by RILEM TC 281-CCC, RILEM Tech Letter 5 (2020) 85–100.
- [6] S. Von Greve-Dierfeld, B. Lothenbach, A. Vollpracht, et al., Understanding the carbonation of concrete with supplementary cementitious materials: a critical review by RILEM TC 281-CCC, Mater Struct 53 (2020) 136, <https://doi.org/10.1617/s11527-020-01558-w>.
- [7] M. Stefanoni, U. Angst, B. Elsener, Corrosion rate of carbon steel in carbonated concrete – A critical review, Cement and Concrete Research 103 (2018) 35–48.
- [8] DA. Ramirez, G.R. Meira, M. Quattrone, M.J. Vanderley, A review on reinforcement corrosion propagation in carbonated concrete – Influence of material and environmental characteristics, Cement and Concrete Composites 140 (2023), <https://doi.org/10.1016/j.cemconcomp.2023.105085>.
- [9] F. Lollini, E. Redaelli, Corrosion rate of carbon steel in carbonated concrete made with different supplementary cementitious materials, Corrosion Engineering, Science and Technology 56 (5) (2021) 473–482, <https://doi.org/10.1080/1478422X.2021.1916236>.
- [10] NS-EN 450-1:2012 Fly ash for concrete — Part 1: Definition, specifications and conformity criteria.
- [11] K. De Weerd, G. Plusquellec, A.B. Revert, M.R. Geiker, B. Lothenbach, Effect of carbonation on the pore solution of mortar, Cement and Concrete Research 118 (2019) 38–56, <https://doi.org/10.1016/j.cemconres.2019.02.004>.
- [12] ASTM C618-22, Standard Specification for Coal Fly Ash and Raw or Calcined Natural Pozzolan for Use in Concrete.
- [13] https://www.sement.heidelbergmaterials.no/no/Standard_FA.
- [14] NS-EN 1992 Eurocode 2 – Design of concrete structures – Part 1-1: General rules and rules for buildings.
- [15] A.B. Revert, K. De Weerd, K. Hornbostel, M.R. Geiker, Carbonation-induced corrosion: Investigation of the corrosion onset, Construction and Building Materials 162 (2018), <https://doi.org/10.1016/j.conbuildmat.2017.12.066>.

- [16] C. Andrade, V. Castelo, C. Alonso, J. González, The Determination of the Corrosion Rate of Steel Embedded in Concrete by the Polarization Resistance and AC Impedance Methods, *ASTM International* 20 (1986).
- [17] M. Stern, A.L. Geary, Theoretical Analysis of the Shape of Polarization Curves, *Journal of the Electrochemical Society* 104 (1957) 7.
- [18] A.B. Revert, K. De Weerd, J.U. Jakobsen, M.R. Geiker, Impact of Accelerated Carbonation on Microstructure and Phase Assemblage, *Nordic Concrete Research* 59 (1) (2018) 111–126, <https://doi.org/10.2478/ncr-2018-0018>.
- [19] A. Leemann, F. Moro, Carbonation of concrete: the role of CO₂ concentration, relative humidity and CO₂ buffer capacity, *Materials and Structures* 50 (2018), <https://doi.org/10.1617/s11527-016-0917-2>.
- [20] A.B. Revert, K. De Weerd, K. Hornbostel, M.R. Geiker, Carbonation Characterization of Mortar with Portland Cement and Fly Ash, Comparison of Techniques, *Nordic Concrete Research* 54 (2016) 60–76.
- [21] A. Köliö, M. Honkanen, J. Lahdensivu, M. Vippola, M. Pentti, Corrosion products of carbonation induced corrosion in existing reinforced concrete facades, *Cem. Concr. Res.* 78 (Part B) (2015) 200–207.
- [22] U.M. Angst, M.R. Geiker, A. Michel, et al., The steel–concrete interface, *Mater Struct* 50 (2017) 143, <https://doi.org/10.1617/s11527-017-1010-1>.
- [23] R. Zhang, A. Castel, R. François, Influence of steel–concrete interface defects owing to the top-bar effect on the chloride-induced corrosion of reinforcement, *Mag. Concr. Res.* 63 (2011) 773–781.
- [24] A.B. Revert, K. Hornbostel, K. De Weerd, M.R. Geiker, Macrocell corrosion in carbonated Portland and Portland-fly ash concrete - Contribution and mechanism, *Cement and Concrete Research* 116 (2019), <https://doi.org/10.1016/j.cemconres.2018.12.005>.
- [25] C. Andrade, C. Alonso, J. Gulikers, et al., RILEM TC-154-EMC: "Electrochemical techniques for measuring metallic corrosion" Test methods for on-site corrosion rate measurement of steel reinforcement in concrete by means of the polarization resistance method, *Mater Struct* 37 (2004) 623–643.
- [26] Bertolini, B. Elsener, P. Pedferri, E. Redaelli, R. Polder, *Corrosion of Steel in Concrete*, Wiley-VCH Verlag GmbH & Co, Weinheim, Germany, 2013.
- [27] ASTM C 876–91, Standard Test Method for Half-Cell Potential of Reinforcing Steel in Concrete, ASTM, West Conshohocken, PA, USA, 1991.
- [28] John P. Broomfield, *Corrosion of Steel in Concrete. Understanding, Investigation and Repair*, 3rd edition, CRC press, 2023.